2008

Raman study on the effects of sintering temperature on the Jc(H) performance of MgB2 superconductor

W. X. Li
Shanghai University

R. H. Chen
Shanghai University

Y. Li
Shanghai University

M. Y. Zhu
Shanghai University

H. M. Jin
Shanghai University

See next page for additional authors

Raman study on the effects of sintering temperature on the $J_c(H)$ performance of MgB_2 superconductor

W. X. Li,[a] R. H. Chen,[a] Y. Li, M. Y. Zhu, and H. M. Jin
School of Materials Science and Engineering, Shanghai University, 149 Yanchang Rd., Shanghai 200072, People's Republic of China

R. Zeng and S. X. Dou[b]
Institute for Superconducting and Electronic Materials, University of Wollongong, Wollongong, New South Wales 2522, Australia

B. Lu
Instrumental Analysis and Research Center, Shanghai University, 99 Shangda Rd., Shanghai 200444, People's Republic of China

(Received 31 August 2007; accepted 7 November 2007; published online 14 January 2008)

The influence of sintering temperature on the critical transition temperature T_c and critical current density J_c for the MgB_2 superconductor was investigated systematically with the observation of Raman scattering measurement and flux pinning force F_p analysis. The enhanced E_{2g} mode in Raman spectra with increasing *in situ* sintering temperature shows gradual strengthening of the electron-phonon coupling in MgB_2, which means that the crystals become more harmonic after higher temperature sintering. However, the crystal harmonicity is degraded for samples sintered at even higher temperature due to Mg deficiency. A possible explanation for the $J_c(H)$ performance, which is in accordance with the Raman spectroscopy observation and F_p analysis, is the cooperation between the electron-phonon coupling in the E_{2g} mode and the flux pinning centers, mainly originating from the lattice distortion due to the different sintering temperatures. © *2008 American Institute of Physics*. [DOI: 10.1063/1.2829808]

I. INTRODUCTION

Due to the surprisingly high critical temperature for a binary system (T_c=39 K) and the lack of weak link effects, the discovery of superconductivity in MgB_2 has attracted intense scientific interest worldwide.[1] A variety of experimental measurements, including those on the isotope effect[2] and the T_c pressure dependence,[3] have indicated that MgB_2 is a phonon-mediated superconductor. In particular, the significant boron isotope effect[2,4] ($\alpha_B=-d\ln T_c/d\ln M_B=0.26\pm0.03$, where M_B is the mass of boron) and the small magnesium isotope effect[4] ($\alpha_{Mg}=0.02\pm0.01$) suggest that electron-phonon coupling plays an important role in the pairing mechanism. Further research has found that MgB_2 exhibits a rich multiple-band structure, which has been observed by a number of experimental techniques, such as angle-resolved photoemission spectroscopy, the de Haas–van Alphen effect, and the Hall resistivity.[5–7] These results confirm previous band structure calculations[8,9] and reveal strongly two-dimensional $sp_xp_y(\sigma)$ bands, as well as three-dimensional $p_z(\pi)$ bands. Owing to the simple hexagonal structure (space group $P6/mmm$), four optical modes at the Γ point of the Brillouin zone are predicted for MgB_2: a silent B_{1g} mode (at 87.1 meV, ≈700 cm^{-1}), the E_{2g} Raman mode (at 74.5 meV, ≈600 cm^{-1}), and the infrared active E_{2u} (at 40.7 meV, ≈330 cm^{-1}), and A_{2u} (at 49.8 meV, ≈400 cm^{-1}) modes, where only the E_{2g} mode is Raman active and strong coupling to the electronic conduction σ bands is predicted. The optical E_{2g} phonon has been found theoretically to lie in the frequency region 515–665 cm^{-1},[8,10,11] and the broad feature observed in the Raman spectra of pure MgB_2 around 600 cm^{-1} (width ~300 cm^{-1}) has been attributed to this mode.[10,12–14] The significant broadening of this Raman peak arises mainly from the exceptionally strong electron-phonon coupling of the E_{2g} mode to the partially occupied planar boron σ bands near the Fermi surface,[11,15] which is due to their large anharmonicities.[11,16] Since the lattice distortion is one of the most important factors to influence the critical current density $J_c(H)$ it is expected that the changes in the Raman spectra due to the different material processing conditions may reflect changes in the superconducting properties of MgB_2.

However, the influences of the different sintering temperatures on the band variation and structure are not well understood from a fundamental point of view, but are known to be related to the critical current density $J_c(H)$.[17,18] To confirm the physical mechanism of the $J_c(H)$ variation and the origin of the flux pinning force, $F_p=-J_cH$, with different sintering temperatures, Raman scattering measurements were employed in this study. Raman scattering has the benefits of excellent energy resolution, a relatively large penetration depth, the ability to selectively measure different portions of the Fermi surface(s),[19] and, especially in superconductors, the benefit of revealing both the existence of the superconducting gap and its strong coupling to some of the active Raman phonons.[20] On the basis of the flux pinning force

[a]Also at Institute for Superconducting and Electronic Materials, University of Wollongong, Wollongong, NSW 2522, Australia.
[b]Author to whom correspondence should be addressed. Electronic mail: shi@uow.edu.au.

mechanism, it is possible that the $J_c(H)$ behavior can be effectively studied by rapid and convenient Raman spectroscopy to gain better insight into the mechanism that controls the $J_c(H)$.

II. EXPERIMENTAL DETAILS

MgB_2 superconductor bulks were prepared by an *in situ* reaction process using mixed powders of micron size magnesium (99%) and nanosize amorphous boron (99.99%). The mixtures were ground sufficiently using an agate mortar in an argon gas filled glovebox and pressed into bulks with dimensions of 10 mm in diameter and about 5 mm in thickness under a pressure of ~600 MPa. Then the samples were sintered in a tube furnace at 650, 750, 850, and 950 °C, respectively, for 30 min, at a heating rate of 5 °C/min, and furnace cooled to room temperature. High purity argon gas flow was maintained throughout the sintering process.

All samples were characterized by x-ray diffraction (XRD) (D\max-2200) and field emission gun scanning electron microscopy (JSM-6700F). The crystal structure was refined with the aid of JADE 5.0 software. The Raman scattering was measured by a confocal laser Raman spectrometer (Renishaw inVia plus) with a 100× microscope. The 514.5 nm line of an Ar^+ laser was used for excitation, with the laser power maintained at about 20 mW, measured on the laser spot on the samples, in order to avoid laser heating effects on the studied materials. Several spots were selected on the same sample to collect the Raman signals in order to make sure that the results were credible. The magnetization was measured at 5 and 20 K using a physical properties measurement system (Quantum Design) in a time-varying magnetic field with sweep rate of 50 Oe/s and amplitude of 8.5 T. The magnetic J_c was derived from the height of the magnetization loop ΔM using the Bean model: $J_c=20\Delta M/[a(1-a/3b)]$, where a and b are the dimensions of the sample perpendicular to the direction of the measurement field, with $a<b$. J_c versus magnetic field was measured up to 8.5 T. The magnetoresistivity $\rho(H,T)$ was measured with H applied perpendicular to the current direction, using the four probe method in the temperature range from 4.2 to 300 K and the field range from 0 to 9 T. The T_c, irreversibility field H_{irr}, and upper critical field H_{c2} can be deduced from $\rho(H,T)$.

III. RESULTS AND DISSCUSSION

Figure 1 contains the normalized ambient Raman spectra of MgB_2 sintered at 650, 750, 850, and 950 °C for 30 min. There are two peaks in the measurement range from 250 to 1000 cm^{-1} centered at about 560–580 and 750–790 cm^{-1}, respectively. The electron-phonon coupling intensity and crystal distortion will influence the Raman shift and the linewidth of the Raman scattering, which can give some insight into the anharmonicity/harmonicity competition of the E_{2g} mode. The broad peaks at 560–580 cm^{-1}, associated with the E_{2g} mode, shift to high frequency with increasing sintering temperature, and the full width at half maximum (FWHM) of these peaks shows an increasing trend, too. In the theoretical calculations on the *ab initio* band structure to describe the electron-phonon coupling between the electronic bands and the phonon E_{2g} mode in MgB_2, the frequency of the harmonic E_{2g} mode is located at 600 cm^{-1}.[21] Some experimental researches on the temperature dependence of the Raman spectra also indicate that the intensity of the E_{2g} shape weakens with gradually decreasing temperature.[22,23] The difference is that the E_{2g} mode shifts to higher frequency and becomes sharp for strong intensity, while the linewidth becomes narrow. The most harmonic E_{2g} mode in this research is located at 581 cm^{-1} with a broad FWHM of 285 cm^{-1} for the sample sintered at 850 °C. The great linewidth of the E_{2g} mode used to be attributed to anharmonic effects in the previous literature,[10–12,22,24,25] which seems to contradict the trend of the frequency shift in this research. Theoretical calculations have demonstrated that the Raman data can be explained if dynamical effects beyond the adiabatic Born-Oppenheimer approximation and electron lifetime effects are included in the phonon self-energy, without invoking anharmonicity.[26] This is consistent with the later harmonic phonon dispersion results[27,28] obtained from inelastic x-ray scattering.[27,29,30]

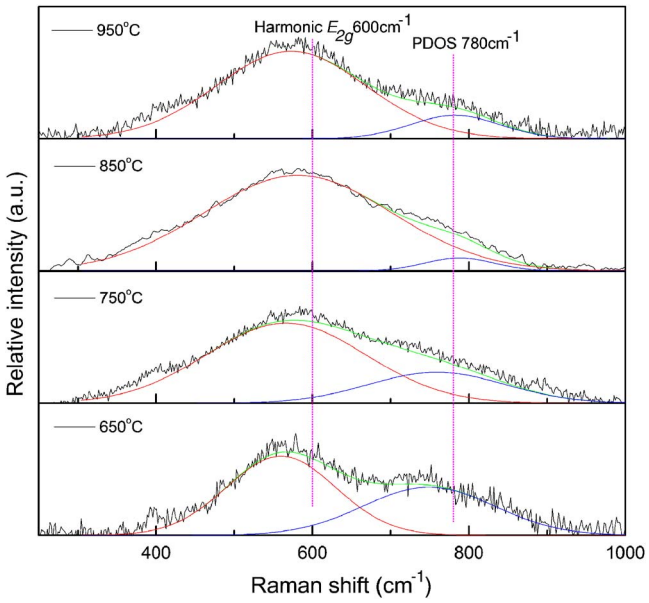

FIG. 1. (Color online) Normalized Raman spectra with Gaussian fitted E_{2g} mode and PDOS distortion for MgB_2 sintered at 650, 750°, 850, and 950 °C. The base lines have been subtracted from the patterns.

As for the MgB_2 synthesized at the different temperatures, there are a number of defects both in and between the crystals. Eisterer *et al.* have researched the influence of disorder on the superconducting properties of MgB_2 wires and extracted the mean free path of the charge carriers in the σ band from the Gofkov-Goodman relation.[31] The wires fall in the range from moderately clean to the dirty limit, and the increase in the upper critical field (H_{c2}) with increasing disorder leads to higher critical currents in high magnetic fields. In this study, the peaks centered at 750–790 cm^{-1} are understood to arise from sampling of the phonon density of states (PDOS) due to disorder.[10,11,32] In disordered systems, relaxation of the q-selection rules may occur, leading to Brillouin zone folding and consequently to the appearance in the Raman spectrum of additional features connected with phonons lying beyond the zone center. Hence, the PDOS in anhar-

TABLE I. The properties of MgB_2 sintered at 650, 750, and 950 °C.

Annealing (°C min)	Lattice parameters		$\frac{I^{220}_{MgO}}{I^{101}_{MgB_2}}$(%)[a]	T_c (K)	H_{irr} (25 K) (T)	H_{c2} (25 K) (T)	ρ ($\mu\Omega$ cm) (40 K)	ρ ($\mu\Omega$ cm) (300 K)	RRR
	a(Å)	c(Å)							
650×30	3.08505	3.52620	4.9	36.8	5.9	8.7	70.8	138.7	1.96
750×30	3.08496	3.52610	5.6	37.3	5.7	8.0	58.1	120.3	2.07
850×30	3.08489	3.52540	5.4	37.8	5.3	6.8	42.2	91.4	2.16
950×30	3.08355	3.52175	4.7	38.3	5.0	6.2	27.1	62.2	2.29

[a]The ratio calculated from the (2 2 0) peaks of MgO and the (1 0 1) peaks of MgB_2.

monic MgB_2 is very broad, and its frequency changes greatly with sintering temperature. As shown in Fig. 1, the samples sintered at lower and higher temperatures display strong defects due to defective crystal growth and the Mg deficiency caused by evaporation, respectively. Note that this PDOS peak of the sample sintered at 850 °C is folded into the E_{2g} mode for these relatively harmonic crystals.

The other properties also show the trend that the crystals become more harmonic with increased sintering temperature. Table I show the measured data for the MgB_2 sintered for 30 min under a series of processing temperatures: 650, 750, 850, and 950 °C. The lattice parameters calculated from XRD patterns show the sintering temperature effects on the MgB_2 crystals. The normal state resistivity at 300 K decreases with increasing processing temperature, indicating that the grains grow more perfectly with enlarged intergranular contact areas at higher temperatures. On the other hand, the resistivity behavior near 40 K is attributed to the intragranular defects since, as the temperature decreases, the phonon contribution to the resistivity decreases.[33] Additionally, the increasing residual resistivity ratios (RRRs) $[\rho(300\ \mathrm{K})/\rho(40\ \mathrm{K})]$ are proper evidence for crystalline perfection. At the same time, H_{irr} and H_{c2} decrease for the same reason, as shown in Table I and Fig. 2. The $H_{irr}(T)$ and $H_{c2}(T)$ curves are steeper for the samples sintered at lower temperatures, which is in accordance with the variation of resistivities at 40 K. As a result, the T_c of MgB_2 increases steadily with increasing sintering temperatures as the crystallinity is improved. The liquid Mg that is present in high temperature sintering makes crystallization easier and more satisfactory. It can be deduced from these characteristics that considerable lattice distortion exists in the samples that were sintered at low temperature due to inefficient crystallization.

The dependences of the peak center, relative intensity, and FWHM on the sintering temperature for the E_{2g} mode and PDOS distortion of all the samples are presented in Fig. 3. The relative intensity of the E_{2g} mode shifts to harmonic behavior with increased sintering temperature, while the intensity of the PDOS distortion becomes weak. This indicates that the crystal distortion tends to decrease with the decreased lattice volume. Although the sample sintered at 950 °C should theoretically be more harmonic than any other sample, its crystallinity was degraded by the inevitable evaporation of Mg due to the high partial pressure when the sintering temperature exceeds 900 °C, so its E_{2g} mode is weakened, while the distortion of its PDOS has become much stronger. The sample sintered at 850 °C is the most harmonic one, as indicated by its strong E_{2g} mode at a frequency of 581 cm^{-1}, combined with a large linewidth (285 cm^{-1}) and by its weak disorder Raman response peak centered at 788 cm^{-1}, with a small linewidth of 104 cm^{-1}; however, its $J_c(H)$ performance is worse than those of the samples sintered at 650, 750, and 950 °C, as shown in Fig. 4. The critical currents are generally high in weak fields and low temperatures, but the $J_c(H)$ of all the samples shows flux jumping when the measurement fields are less than 2.2 T at 5 K. The sample sintered at 750 °C shows the highest $J_c(H)$ performance due to both the strong electron-phonon coupling induced by the intense E_{2g} mode at a frequency of

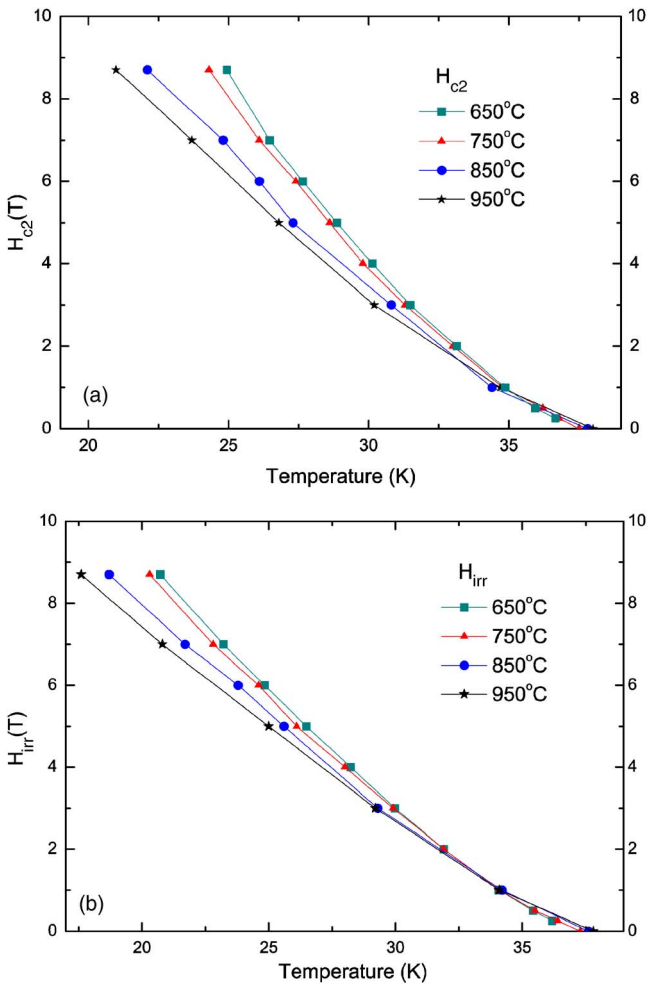

FIG. 2. (Color online) (a) The irreversibility field H_{irr} and (b) upper critical field H_{c2} as a function of temperature for MgB_2 sintered at 650, 750, 850, and 950 °C.

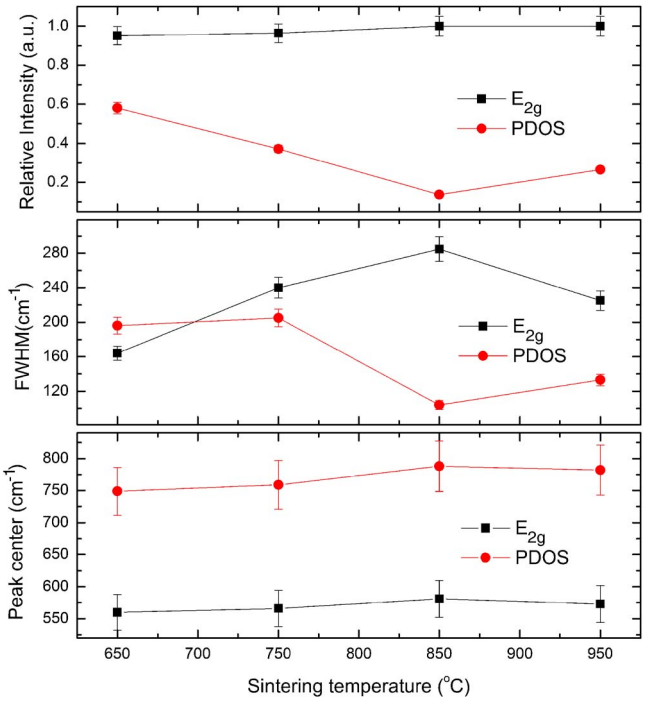

FIG. 3. (Color online) Dependence of the relative intensity, the FWHM, and the peak center of the E_{2g} mode and PDOS distortion on the sintering temperature for MgB_2 sintered at 650, 750, 850, and 950 °C.

(566 cm^{-1}), which also has a large linewidth (240 cm^{-1}), and the large crystal disorder, which is indicated by a peak at the frequency of 759 cm^{-1} with a linewidth of 205 cm^{-1}, as shown in Figs. 1 and 3. The sample sintered at 650 °C also shows high $J_c(H)$ performance because this sample is characterized by both a proper E_{2g} mode and great crystal distortion for its large volume distortion.

The flux pinning force at 20 K has been analyzed, with the results shown in Fig. 5 for MgB_2 sintered at different temperatures, in order to study the characteristics of the pinning mechanisms in the undoped Mg–B system. Dew-Hughes[34] has proposed a general expression for the normalized pinning force density in a chemical doping system as follows:

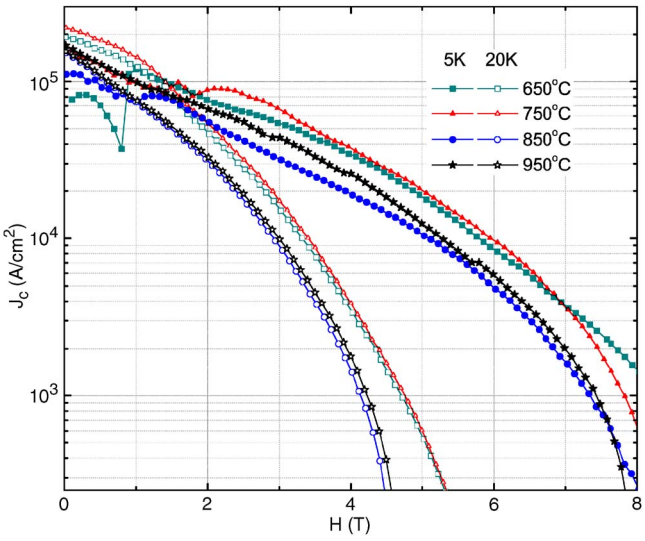

FIG. 4. (Color online) Critical current density $J_c(H)$ at 5 and 20 K of MgB_2 sintered at 650, 750, 850, and 950 °C.

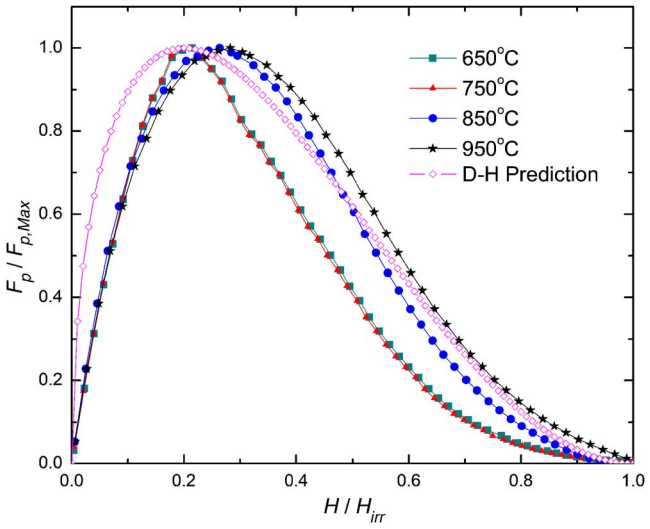

FIG. 5. (Color online) The reduced flux-pinning force, $F_p/F_{p,\max}$, as a function of reduced magnetic field, $H/H_{\rm irr}$, at 20 K for MgB_2 sintered at 650, 750, 850, and 950 °C and for the fitted prediction results of Dew-Hughes formula.

$$F_p(h) = F_p/F_{p,\max} \propto h^p(1-h)^q,$$

where $F_p/F_{p,\max}$ is the normalized pinning force density, $F_{p,\max}$ is the maximum pinning force density, and $h=H/H_{\rm irr}$ is the reduced applied magnetic field. The parameters p and q are constants according to different pinning mechanisms. Six different pinning cases are developed in describing the elementary pinning using this equation. (a) Normal core pinning, volume pins: $p=0$, $q=2$; (b) Δk pinning, volume pins: $p=1$, $q=1$; (c) normal core pinning, surface pins: $p=1/2$, $q=2$; (d) Δk pinning, surface pins: $p=3/2$, $q=1$; (e) normal core pinning, point pins: $p=1$, $q=2$; and (f) Δk pinning, point pins: $p=2$, $q=1$. For the MgB_2 sintered at different temperatures, the maximum of the normalized pinning force is around $h=0.2-0.3$, which suits case (c) of normal core pinning and surface pins as shown in Fig. 5. The peaks in the $F_p/F_{p,\max}(h)$ curves of the samples sintered at 850 and 950 °C are located at higher field than those of the samples sintered at 650 and 750 °C because of the low $H_{\rm irr}$ arising from the perfect crystallization. According to the Raman research, it is believed that the $J_c(H)$ of the samples sintered at 850 and 950 °C is determined by the grain boundaries existing in MgB_2 matrix and a little amount of MgO inclusions. The small peak shift for the sample sintered at 950 °C is caused by the improved crystal connection for the higher sintering temperature. It means that the $J_c(H)$ values of them depends more on the grain boundaries, inclusions, and defects. Whereas, the shift of the peak in the $F_p/F_{p,\max}(h)$ curves toward the lower field region may be regarded as a consequence of the enhanced $H_{\rm irr}$ for MgB_2 sintered at low temperatures with great lattice distortion. Although the grain boundaries are believed as the flux pinning centers in the previous researches, the crystal distortion is also one of the most dominant factor of high $J_c(H)$ performance in MgB_2 superconductor. In consideration of the high $J_c(H)$ behavior of the samples sintered at 650 and 750 °C, it can be deduced that large crystal disorder is even more important than grains boundary's contribution to the high $J_c(H)$ performance of

MgB_2 superconductor. This is because the crystal distortions are the origin of most stress-induced flux pinning centers. An ideal condition for perfect $J_c(H)$ performance is the coexistence of intense E_{2g} mode, abundant grain boundary and significant crystal distortion in polycrystalline MgB_2.

IV. CONCLUSION

Summarizing, the influence of the superconducting properties of MgB_2 can be predicted by Raman scattering measurements, as both the intensity of its E_{2g} mode and the crystal distortion can be observed in the Raman spectra. The strength of the electron-phonon coupling, which is related to the E_{2g} mode at the Γ point of the Brillouin zone, is the dominant factor that will determine the T_c of MgB_2. On the other hand, the Raman scattering measurements and F_p analysis indicate that the intense crystal distortion, which is the origin of most stress-induced flux pinning centers, is the dominant factor for the high $J_c(H)$ performance in MgB_2 superconductor. The samples sintered at 650 and 750 °C show high $J_c(H)$ for the perfect conjunction of proper intensity of the E_{2g} mode, grain boundary, and crystal distortion during the crystallization, while the samples sintered at high temperatures show low $J_c(H)$ for lack of crystal distortion. Furthermore, technologies that can strengthen the E_{2g} mode and afford enough crystal distortion in MgB_2 at the same time will be the most promising methods to enhance the superconducting performance of this material.

ACKNOWLEDGMENTS

The authors are grateful to Dr. T. Silver for fruitful discussion. The authors also thank the Natural Science Foundation of China (Grant No. 50471100), the Australian Research Council, Hyper Tech Research, Inc., and CMS Alphatech International Ltd. for their financial support.

[1] J. Nagamatsu, N. Nakagawa, T. Muranaka, Y. Zenitani, and J. Akimitsu, Nature (London) **410**, 63 (2001).
[2] S. L. Bud'ko, G. Lapertot, C. Petrovic, C. E. Cunningham, N. Anderson, and P. C. Canfield, Phys. Rev. Lett. **86**, 1877 (2001).
[3] T. Vogt, G. Schneider, J. A. Hriljac, G. Yang, and J. S. Abell, Phys. Rev. B **63**, 220505 (2001).
[4] D. G. Hinks, H. Claus, and J. D. Jorgensen, Nature (London) **411**, 457 (2001).
[5] H. Uchiyama, K. M. Shen, S. Lee, A. Damascelli, D. H. Lu, D. L. Feng, Z. X. Shen, and S. Tajima, Phys. Rev. Lett. **88**, 157002 (2002).
[6] E. A. Yelland, J. R. Cooper, A. Carrington, N. E. Hussey, P. J. Meeson, S. Lee, A. Yamamoto, and S. Tajima, Phys. Rev. Lett. **88**, 217002 (2002).
[7] Y. Eltsev, K. Nakao, S. Lee, T. Masui, N. Chikumoto, S. Tajima, N. Koshizuka, and M. Murakami, Phys. Rev. B **66**, 180504(R) (2002).
[8] J. Kortus, I. I. Mazin, K. D. Belashchenko, V. P. Antropov, and L. L. Boyer, Phys. Rev. Lett. **86**, 4656 (2001).
[9] J. M. An and W. E. Pickett, Phys. Rev. Lett. **86**, 4366 (2001).
[10] K. P. Bohnen, R. Heid, and B. Renker, Phys. Rev. Lett. **86**, 5771 (2001).
[11] T. Yildirim, O. Gulseren, J. W. Lynn, C. M. Brown, T. J. Udovic, Q. Huang, N. Rogado, K. A. Regan, M. A. Hayward, J. S. Slusky, T. He, M. K. Haas, P. Khalifah, K. Inumaru, and R. J. Cava, Phys. Rev. Lett. **87**, 037001 (2001).
[12] J. Hlinka, I. Gregora, J. Pokorny, A. Plecenik, P. Kus, L. Satrapisky, and S. Benacka, Phys. Rev. B **64**, 140503 (2001).
[13] A. F. Goncharov, V. V. Struzhkin, E. Gregoryanz, J. Hu, R. J. Hemley, H. Mao, G. Lapertot, S. L. Bud'ko, and P. C. Canfield, Phys. Rev. B **64**, 100509 (2001).
[14] K. P. Meletov, M. P. Kulakov, N. N. Kolesnikov, J. Arvanitidis, and G. A. Kourouklis, JETP Lett. **75**, 406 (2002).
[15] I. Loa and K. Syassen, Solid State Commun. **118**, 279 (2001).
[16] K. Kunc, I. Loa, K. Syassen, R. K. Kremer, and K. Ahn, J. Phys.: Condens. Matter **13**, 9945 (2001).
[17] J. H. Kim, S. X. Dou, J. L. Wang, D. Q. Shi, X. Xu, M. S. A. Hossain, W. K. Yeoh, S. Choi, and T. Kiyoshi, Supercond. Sci. Technol. **20**, 448 (2007).
[18] W. K. Yeoh, J. Horvat, J. H. Kim, X. Xu, and S. X. Dou, Appl. Phys. Lett. **90**, 122502 (2007).
[19] J. W. Quilty, S. Lee, and S. Tajima, Phys. Rev. Lett. **90**, 207006 (2003).
[20] M. Cardona, Physica C **317–318**, 30 (1999).
[21] P. M. Rafailov, S. Bahrs, and C. Thomsen, Phys. Status Solidi B **226**, R9 (2001).
[22] L. Shi, H. R. Zhang, L. Chen, and Y. Feng, J. Phys.: Condens. Matter **16**, 6541 (2004).
[23] J. W. Quilty, S. Lee, A. Yamamoto, and S. Tajima, Phys. Rev. Lett. **88**, 087001 (2002).
[24] H. Martinho, C. Rettori, P. G. Pagliuso, A. A. Martin, N. O. Moreno, and J. L. Sarrao, Solid State Commun. **125**, 499 (2003).
[25] D. Di Castro, E. Cappelluti, M. Lavagnini, A. Sacchetti, A. Palenzona, M. Putti, and P. Postorino, Phys. Rev. B **74**, 100505 (2006).
[26] M. Calandra, M. Lazzeri, and F. Mauri, Physica C **456**, 38 (2007).
[27] A. Shukla, M. Calandra, M. d'Astuto, M. Lazzeri, F. Mauri, C. Bellin, M. Krisch, J. Karpinski, S. M. Kazakov, J. Jun, D. Daghero, and K. Parlinski, Phys. Rev. Lett. **90**, 095506 (2003).
[28] Y. Kong, O. V. Dolgov, O. Jepsen, and O. K. Andersen, Phys. Rev. B **64**, 020501(R) (2001).
[29] M. d'Astuto, M. Calandra, S. Reich, A. Shukla, M. Lazzeri, F. Mauri, J. Karpinski, N. D. Zhigadlo, A. Bossak, and M. Krisch, Phys. Rev. B **75**, 174508 (2007).
[30] A. Q. R. Baron, H. Uchiyama, Y. Tanaka, S. Tsutsui, D. Ishikawa, S. Lee, R. Heid, K.-P. Bohnen, S. Tajima, and T. Ishikawa, Phys. Rev. Lett. **92**, 197004 (2004).
[31] M. Eisterer, R. Müller, K. Schöppl, H. W. Weber, S. Soltanian, and S. X. Dou, Supercond. Sci. Technol. **20**, S.117 (2007).
[32] R. Osborn, E. A. Goremychkin, A. I. Kolesnikov, and D. G. Hinks, Phys. Rev. Lett. **87**, 017005 (2001).
[33] J. M. Rowell, Supercond. Sci. Technol. **16**, R17 (2003).
[34] D. Dew-Hughes, Philos. Mag. **30**, 293 (1974).